MOLECULAR AND CELLULAR BIOLOGY, June 2010, p. 3016–3026 Vol. 30, No. 12
0270-7306/10/$12.00 doi:10.1128/MCB.01591-09

Genetic Analysis of Cytoprotective Functions Supported by Graded Expression of Keap1▽

Keiko Taguchi,[1] Jonathan M. Maher,[1] Takafumi Suzuki,[1] Yukie Kawatani,[1] Hozumi Motohashi,[2] and Masayuki Yamamoto[1]*

Department of Medical Biochemistry[1] and Center for Radioisotope Sciences,[2] Tohoku University Graduate School of Medicine, 2-1 Seiryo-cho, Aoba-ku, Sendai 980-8575, Japan

Received 11 December 2009/Returned for modification 2 February 2010/Accepted 10 April 2010

Keap1 regulates Nrf2 activity in response to xenobiotic and oxidative stresses. Nrf2 is an essential regulator of cytoprotective genes. *Keap1*-null mice are lethal by weaning age due to malnutrition caused by severe hyperkeratosis of the upper digestive tract. Analysis of *Keap1*::*Nrf2* double mutant mice revealed that currently recognizable phenotypes of *Keap1*-null mice are all attributable to constitutive activation of Nrf2. We previously reported that hepatocyte-specific *Keap1* knockout (*Keap1*$^{flox/-}$::*Albumin*-Cre) mice are viable and more resistant to acute toxicity of acetaminophen (APAP). In the current study, we found that the floxed *Keap1* allele is hypomorphic and that Keap1 expression was decreased in all examined tissues of *Keap1*$^{flox/-}$ mice. Taking advantage of the hypomorphic phenotype of *Keap1*$^{flox/-}$ mice, we examined the effects of graded reduction of Keap1 expression in adult mice. When challenged with APAP, *Keap1*$^{flox/-}$ mice were more protected from mortality than wild-type and even *Keap1*$^{flox/-}$::*Albumin*-Cre mice. In contrast, a decrease in Keap1 levels to less than 50% resulted in increased mortality in a study of 2-year-old mice. These results support our contention that the benefits of Nrf2 activation in acute toxicity are hormetic and that constitutive Nrf2 activation beyond a certain threshold is rather disadvantageous to long-term survival.

Keap1 is a cytoplasmic protein that serves as a substrate adaptor molecule for Cullin-3 (Cul-3)-based ubiquitin E3 ligase (15, 20). The most biologically relevant substrate of Keap1 is Nrf2, which belongs to the CNC (Cap'n'collar) transcription factor family and serves as a master regulator of phase II detoxification and anti-oxidative stress enzymes/proteins (14). Under homeostatic conditions, Keap1 suppresses Nrf2 activity by promoting ubiquitination of Nrf2 and subsequent degradation by the proteasome. Upon exposure to electrophiles, Keap1 activity declines and Nrf2 ubiquitination is halted, leading to nuclear accumulation of Nrf2, which activates the expression of Nrf2 target genes, including many cytoprotective genes (reviewed in references 17, 29, and 38). The Nrf2 protein turns over quite rapidly (16), and Keap1 plays a critical role in degrading Nrf2. Through this function, Keap1 serves as a crucial component in regulating Nrf2 transcriptional activity (20, 43).

Structural and biochemical analyses have revealed the requirements for efficient ubiquitination of Nrf2 by Keap1 (42). Two molecules of Keap1 form a dimer through their N-terminal BTB domain and associate with a single molecule of Nrf2. Nrf2 uses two motifs, ETGE and DLG, in the N-terminal Neh2 domain for binding to the Keap1 dimer. Each Keap1 molecule uses a β-barrel DC domain in the C-terminal region for binding with Nrf2. The two-site binding seems to be an important requirement for Keap1 to maintain its ubiquitin ligase activity. Biochemical studies also suggest that Keap1 is a sensor protein for electrophilic signals (7, 11, 12, 21, 26). Keap1 is a thiol-rich protein, and electrophiles modify thiol moieties in Keap1. This leads to disturbance of the two-site binding structure and results in the decline of ubiquitin ligase activity.

Nrf2 plays an important role in cellular protection against chemical and environmental insults. Nrf2 is expressed in tissues with frequent exposure to electrophilic stressors, including lung and digestive tract (4, 14). *Nrf2*-null mice are susceptible to a numerous and chemically diverse set of electrophiles and oxidants, including acetaminophen (APAP) (5, 9), diesel exhaust particles (1), dextran sulfate (18), lipopolysaccharide (41), and cigarette smoke (13). Nrf2-mediated protection arises because of a multifaceted response to the insults, including the induction of (i) cystine transporter and enzymes for glutathione production, (ii) enzymes metabolizing oxidative intermediates, such as NAD(P)H:quinone oxidoreductase 1 (NQO1), (iii) conjugating enzymes, such as UDP-glucuronosyltransferases (UGT), that increase the hydrophilicity of chemicals, and (iv) ATP-dependent (ATP-binding cassette) transporters, such as multidrug resistance-associated proteins (MRP), that aid in the elimination of toxic metabolites. Our recent study demonstrated that Nrf2 directly regulates several MRP members (28). Thus, enhancement of Nrf2 activity is expected to be beneficial and to strengthen the cytoprotective potential.

We previously knocked out the *Keap1* gene in mice through homologous recombination. In the knockout mice, Nrf2 constitutively accumulated in nuclei, and Nrf2 target genes were constitutively activated (43). However, *Keap1*-null mice were lethal at weaning age due to hyperkeratosis in the upper digestive tract, which leads to obstructive lesions (29, 43). Their body weight gain was retarded, and abnormal metabolic parameters were observed because of malnutrition (45). Impor-

* Corresponding author. Mailing address: Department of Medical Biochemistry, Graduate School of Medicine, Tohoku University, 2-1 Seiryo-cho, Aoba-ku, Sendai, Miyagi, 980-8575, Japan. Phone: 81-22-717-8084. Fax: 81-22-717-8090. E-mail: masiyamamoto@m.tains.tohoku.ac.jp.

▽ Published ahead of print on 19 April 2010.

tantly, these detectable *Keap1*-null phenotypes were all canceled in the double mutant mice that were null for the *Keap1* and *Nrf2* genes, indicating that *Keap1*-null phenotypes are the consequence of the constitutive activation of Nrf2 (43).

To verify the notion that constitutive enhancement of Nrf2 activity is beneficial, we then generated floxed alleles of the *Keap1* gene and performed hepatocyte-specific deletion of the *Keap1* gene by crossing the floxed-*Keap1* mice with transgenic mice expressing Cre recombinase under the regulation of the *Albumin* gene (*Alb*-Cre mice) (31). This hepatocyte-specific *Keap1* conditional-knockout line of mice displayed constitutive Nrf2 activation in the liver. These mice were highly resistant to APAP-induced toxicity in comparison with control wild-type mice carrying the *Alb*-Cre transgene.

In this study, we carried out a closer examination of the floxed-*Keap1* mice and unexpectedly found that floxation of the *Keap1* allele with *loxP* sites led to a partial disruption of Keap1 expression. *Keap1*$^{flox/flox}$ and *Keap1*$^{flox/-}$ mice displayed reduced expression of Keap1 protein in various tissues, and transgene-derived Keap1 rescued the mice from the knockdown phenotypes. We then utilized the knockdown mice to examine the effects of genetic and constitutive activation of Nrf2 on both short-term survival after chemical toxicity and long-term survival under normal breeding conditions. Consistent with benefits of pharmacological Nrf2 activation that have been described in many different disease models, the reduced expression of Keap1 and subsequent Nrf2 activation confers resistance against acute toxicity on the knockdown mice. However, to our surprise, the constitutive activation of Nrf2 was not beneficial but rather disadvantageous for the long-term survival of these knockdown mice. This study has for the first time challenged and clarified the effects of constitutive and whole-body activation of Nrf2 at several graded levels through exploiting the *Keap1* gene knockdown allele.

MATERIALS AND METHODS

Chemicals. APAP, *N*-acetyl cysteine (NAC), and DL-buthionine-[*S*,*R*]-sulfoximine (BSO) were purchased from Sigma-Aldrich, Inc. (St. Louis, MO). Propylene glycol and Mildform 10N were purchased from Wako Pure Chemical Industries, Ltd. (Osaka, Japan). Isogen and heparin were purchased from Nippon Gene Co., Ltd. (Toyama, Japan) and Mochida Pharmaceutical Co., Ltd. (Tokyo, Japan), respectively. All other chemicals used were obtained from commercial sources and were of the highest grade available.

Mice. Generation of *Keap1*$^{+/-}$ mice (43), *Keap1*$^{flox/+}$ mice (31), *Nrf2*$^{+/-}$ mice (14), and *Keap1* gene regulatory domain (*KRD*)-Keap1 transgenic mice (45) were described previously. Line 34 of *KRD*-Keap1 transgenic mice was used for this study. *Alb*-Cre transgenic mice were purchased from the Jackson Laboratory. *Keratin 5* (*K5*)-Cre transgenic mice were kindly provided by Junji Takeda (39). DNA was taken from each mouse and analyzed by PCR for genotyping. Mice were allowed water and rodent chow *ad libitum*. All mice were kept in specific-pathogen-free conditions and were treated according to the regulations of *The Standards for Human Care and Use of Laboratory Animals of Tohoku University* and *Guidelines for Proper Conduct of Animal Experiments* of the Ministry of Education, Culture, Sports, Science, and Technology of Japan. Mice were killed by cervical dislocation, and tissues were collected and rinsed in phosphate-buffered saline (PBS). Ratios of lean and fat were measured using EchoMR 700 (Aloka Co., Ltd., Tokyo, Japan).

Measurement of cumulative food intake. Male and female mice of the same genotype were separated and put into male and female cages, respectively, after weaning. The food left in the container was weighed every other day, and the average food ingestion per mouse per day was calculated. The cumulative food intake was calculated by summing up these average amounts.

APAP treatment. Seven- to 14-week-old female mice were treated with 700 mg/kg of body weight APAP. APAP was dissolved in 50% propylene glycol at room temperature and intraperitoneally administered to mice at 15 ml/kg. NAC and BSO were coinjected with APAP at 100 mg/kg and 1.6 g/kg, respectively. In the time-course study, mice were sacrificed 48 h after dosing.

RNA purification and real-time PCR. Total RNA was extracted from the forestomach, glandular stomach, and liver using Isogen (Nippon Gene). To prepare total RNA of keratinocytes, the back skin of an 18.5-day embryo (E18.5) was treated with dispase (2.4 mg/ml) at 37°C for 2 h. The peeled epidermis was lysed in Isogen, and total RNA was extracted. cDNA was synthesized using random primers (Life Technologies Corp., Carlsbad, CA). Primers and probes used for amplification of cDNAs of glutamate-cysteine ligase, catalytic subunit (*Gclc*), glutathione peroxidase 1 (*Gpx1*), *Gpx2*, glutathione *S*-transferase A4 (*Gsta4*), *Gstp1*, *Gstp2*, heme oxygenase 1 (*Ho-1*), *Nqo1*, and rRNA are described in Table 1.

Immunoblot analysis. Tissues were homogenized in 9 volumes of 0.25 M sucrose. The 10% homogenate was centrifuged at 600 × *g* for 10 min. The pellet was suspended in 1.6 M sucrose, layered onto a 2 M sucrose bed, and centrifuged at 105,000 × *g* for 60 min. The pellet (nuclear fraction) was suspended in 0.25 M sucrose. Protein concentrations were determined using a bicinchoninic acid (BCA) protein assay kit (Pierce Biotechnology, Rockford, IL). Anti-NQO1 antibody (Abcam plc., Cambridge, United Kingdom), anti-α-tubulin antibody (Sigma-Aldrich, Inc., St. Louis, MO), anti-Keap1 antibody (44), and anti-Nrf2 antibody (28a) were used. Secondary antibodies conjugated with horseradish peroxidase (HRP) were purchased from Zymed Laboratories, Inc. (South San Francisco, CA).

Histological analysis. Tissues were fixed in Mildform 10N and embedded in paraffin for hematoxylin and eosin staining. For immunohistochemical staining, tissues were processed as previously described (45). Samples were treated with the same anti-Nrf2 antibody as the one used in immunoblot analysis. Positive reactivity was visualized through sequential incubation with biotinylated anti-rat IgG, streptavidin-conjugated HRP, and diaminobenzidine (DAB) staining. Hematoxylin was used for nuclear counterstaining.

RESULTS

The floxed *Keap1* allele is hypomorphic. While breeding the mice carrying a floxed allele of the *Keap1* gene, we noticed a slight reduction in the body size of *Keap1*$^{flox/-}$ mice, suggesting that Keap1 expression from the floxed allele might be reduced. Therefore, we examined Keap1 expression in various tissues of the mice carrying the floxed allele (Fig. 1A). We examined *Keap1*$^{flox/flox}$ and *Keap1*$^{flox/-}$ mice together with *Keap1*$^{+/-}$ and wild-type mice and found that Keap1 protein levels were significantly lower in the liver, lung, brain, and kidney of *Keap1*$^{flox/flox}$ and *Keap1*$^{flox/-}$ mice than in these tissues of the wild-type control mice. Other tissues, including stomach, intestine, and spleen, also displayed a marked decrease of the Keap1 protein (data not shown). Consistently, the expression of the Nrf2 target gene *Nqo1* increased in these mice and the increase showed an inverse correlation to the Keap1 abundance in each tissue (Fig. 1A and B). The nuclear accumulation of Nrf2 was clearly increased in all the tissues examined in *Keap1*$^{flox/-}$ mice (Fig. 1C). These results thus indicate that the floxed *Keap1* allele is hypomorphic and that Nrf2 activity is inversely enhanced in *Keap1*$^{flox/flox}$ and *Keap1*$^{flox/-}$ mice. For the sake of simplicity, we refer to the *Keap1*$^{flox/flox}$ and *Keap1*$^{flox/-}$ mice as *Keap1* knockdown mice in this study.

Hyperkeratosis is observed in the esophagus and forestomach of *Keap1* knockdown mice. To verify the systemic effect of decreased production of Keap1 from the floxed allele, we measured body weights and examined histological phenotypes in the upper digestive tracts of *Keap1*$^{flox/-}$ mice. Loss of Keap1 function is known to cause growth retardation and lethality at weaning age due to hyperkeratosis in the esophagus and forestomach (29, 43). At 8 days, the *Keap1*$^{flox/-}$ mice were smaller than littermate *Keap1*$^{flox/+}$ mice and similar in size to *Keap1*-

TABLE 1. Primers and probes used for quantitative PCR

Primer	Sequence
mGclc-F	5′-ATCTGCAAAGGCGGCAAC-3′
mGclc-R	5′-ACTCCTCTGCAGCTGGCTC-3′
mGclc-P	5′-FAM-ACGGGTGCAGCAAGGCCCA-TAMRA-3′
mGpx1-F	5′-CCCGTGCAATCAGTTCGG-3′
mGpx1-R	5′-CCTCAAGTACGTCCGACCT-3′
mGpx1-P	5′-FAM-GGAGAATGGCAAGAATGAAGAGATTCTG-TAMRA-3′
mGpx2-F	5′-TGTCAGAACGAGGAGATCCTG-3′
mGpx2-R	5′-GACTAAAGGTGGGCTGGTACC-3′
mGpx2-P	5′-FAM-CAATACCCTCAAGTATGTCCGACCTG-TAMRA-3′
mGsta4-F	5′-GGGAACAGTATGAGAAGAAGATGCAAAA-3′
mGsta4-R	5′-CCCATCGATTTCAACCAAGG-3′
mGsta4-P	5′-FAM-TGCACACCTGCTTTTCGGCCAAG-TAMRA-3′
mGstp1-F	5′-GCAAATATGTCACCCTCATCTACACC-3′
mGstp1-R	5′-GCAGGGTCTCAAAAGGCTTCA-3′
mGstp1-P	5′-FAM-AGGGCCTTCACGTAGTCATTCTTACCATTCTCATAGT-TAMRA-3′
mGstp2-F	5′-CAAATATGGCACCATGATCTACAGA-3′
mGstp2-R	5′-GCAGGGTCTCAAAAGGCTTCA-3′
mGstp2-P	5′-FAM-AGGGCCTTCACGTAGTCATTCTTACCATTCTCATAGT-TAMRA-3′
mHo1-F	5′-GTGATGGAGCGTCCACAGC-3′
mHo1-R	5′-TTGGTGGCCTCCTTCAAGG-3′
mHo1-P	5′-FAM-CGACAGCATGCCCCAGGATTTGTC-TAMRA-3′
mNqo1-F	5′-AGCTGGAAGCTGCAGACCTG-3′
mNqo1-R	5′-CCTTTCAGAATGGCTGGCA-3′
mNqo1-P	5′-FAM-ATTTCAGTTCCCATTGCAGTGGTTTGGG-TAMRA-3′
rRNA-F	5′-CGGCTACCACATCCAAGGAA-3′
rRNA-R	5′-GCTGGAATTACCGCGGCT-3′
rRNA-P	5′-VIC-TGCTGGCACCAGACTTGCCCTC-TAMRA-3′

null mice (Fig. 2A, upper panel). Even when the pups were fed, the stomachs of *Keap1*$^{flox/-}$ and *Keap1*-null mice were shrunken and contained only small amounts of milk (Fig. 2A, middle panel). The longer diameters of *Keap1*$^{flox/-}$ and *Keap1*-null mouse stomachs were constantly less than half of those of *Keap1*$^{+/-}$ and *Keap1*$^{+/+}$ mouse stomachs. While *Keap1*-null mice died by 14 days, *Keap1*$^{flox/-}$ mice survived longer, albeit they remained smaller than their *Keap1*$^{flox/+}$ littermates (Fig. 2A, lower panel). *Keap1*$^{flox/-}$ mice constantly exhibited lower body weights than wild-type mice (Fig. 2B, and see Fig. 7B). This observation suggests that Keap1 function is substantially defective in *Keap1*$^{flox/-}$ mice, although the phenotype was milder than in *Keap1*-null mice. Hyperkeratosis and hyperplasia of the squamous epithelium were evident in the forestomach and esophagus of *Keap1*$^{flox/-}$ mice (Fig. 2C), as was observed in the upper digestive tracts of *Keap1*-null mice (29, 43). Thus, the floxed *Keap1* allele shows hypomorphic expression of Keap1, but the expression level sustains mice enough to escape lethality at the weaning age.

Transgene-derived Keap1 rescues *Keap1* knockdown mice from hyperkeratosis. We surmised that insertion of the enhanced green fluorescent protein (EGFP) cassette into the 3′ region of the *Keap1* gene (31) might disrupt critical regulatory elements needed for transcription of the *Keap1* gene and reduce the gene expression. To corroborate that the hyperkeratosis observed in *Keap1*$^{flox/-}$ mice is truly caused by the reduced expression of Keap1, we examined whether the transgenic expression of Keap1 rescues the mice from the phenotype. To this end, we utilized a transgenic mouse line expressing Keap1 under the regulation of the *Keap1* gene regulatory domain (*KRD*-Keap1) (45). We crossed *Keap1*$^{flox/flox}$ mice with *Keap1*$^{-/-}$::*KRD*-Keap1 mice and obtained both *Keap1*$^{flox/-}$ mice and *Keap1*$^{flox/-}$::*KRD*-Keap1 mice within a litter. We examined the body weight gain of these mice until 60 days of age and found that *Keap1*$^{flox/-}$::*KRD*-Keap1 mice consistently showed improvement in body weight gain compared to that of *Keap1*$^{flox/-}$ mice, albeit the difference was moderate (Fig. 3A, male mice). We also examined the body weight gain of female *Keap1*$^{flox/-}$::*KRD*-Keap1 and *Keap1*$^{flox/-}$ mice, and the result was reproducible (data not shown). Food intake was also improved in *Keap1*$^{flox/-}$::*KRD*-Keap1 mice, for both males and females (Fig. 3B, upper and lower panel, respectively). The expression levels of *Nqo1* and *Gpx2* in the forestomach and glandular stomach of *Keap1*$^{flox/-}$ mice were significantly decreased in *Keap1*$^{flox/-}$::*KRD*-Keap1 mice, and Nrf2 accumulation was markedly decreased (Fig. 3C and D). Importantly, hyperkeratotic lesions were absent in the forestomach and esophagus of *Keap1*$^{flox/-}$::*KRD*-Keap1 mice (Fig. 3E). Thus, we concluded that the hyperkeratotic lesions were indeed caused by the enfeebled expression of Keap1 and that exogenous Keap1 did correct the abnormalities in *Keap1*$^{flox/-}$ mice.

The *Keap1* deletion in keratinocytes using *K5*-Cre mice results in lethality at the weaning age. We surmise that the most plausible cause of *Keap1*-null mouse lethality is the feeding problem due to severe hyperkeratotic lesions in the upper digestive tract. The abnormal metabolic parameters strongly support this hypothesis (45). However, *Keap1*$^{flox/-}$ mice survived to adulthood, although they suffered from severe esophageal and forestomach hyperkeratosis (Fig. 2). The latter observation implies that there may be some other lesions than those in the upper digestive tract in *Keap1*-null mice that cause the juvenile lethality. To verify or exclude this hypothesis, we carried out keratinocyte-specific disruption of the *Keap1* gene. *Keap1*$^{flox/flox}$ mice were crossed with a transgenic mouse ex-

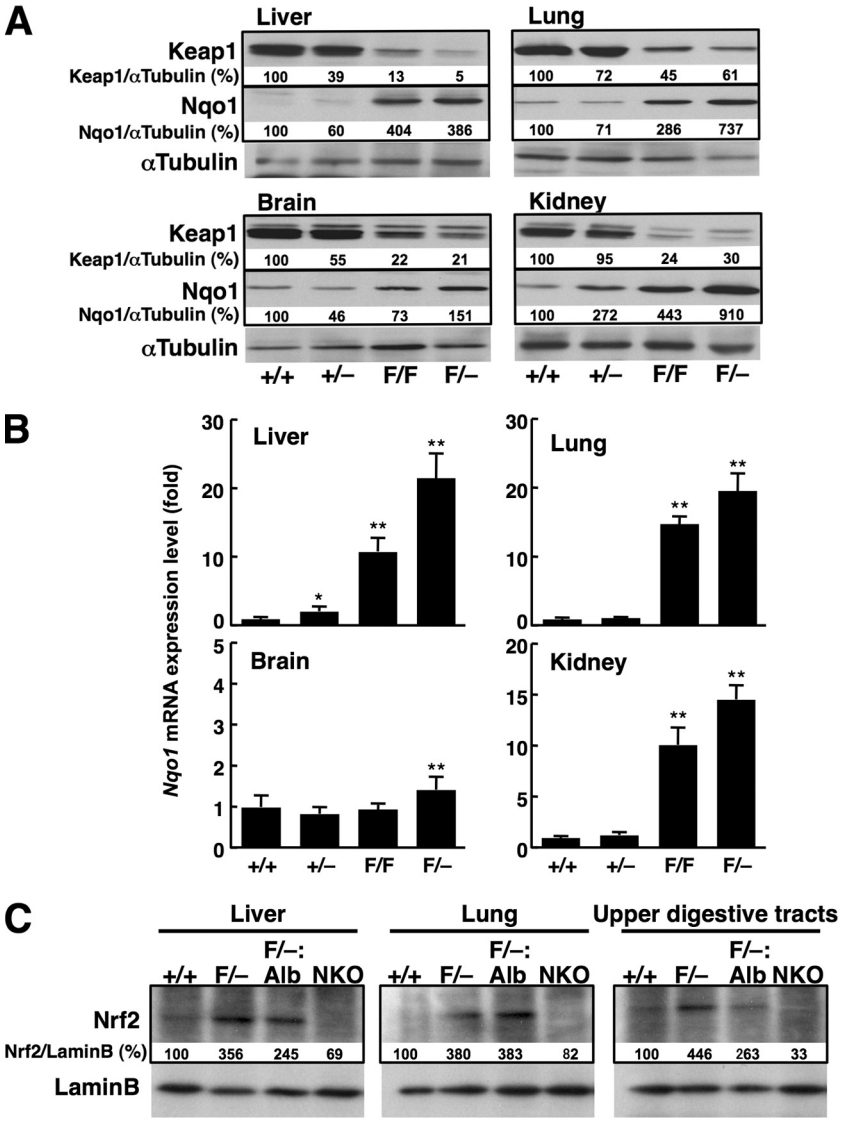

FIG. 1. Expression of Keap1, Nqo1, and Nrf2 in mice carrying floxed *Keap1* alleles. (A) Immunoblot analysis of whole-cell extracts of liver, lung, brain, and kidney with anti-Keap1 and anti-Nqo1. α-Tubulin was detected as a loading control. Band intensities of Keap1 and Nqo1 were quantified and normalized to the band intensity of α-tubulin. The values obtained are shown below the bands of Keap1 or Nqo1. (B) *Nqo1* mRNA expression in liver, lung, brain, and kidney was examined by quantitative reverse transcription-PCR. Ten- to 12-week-old female mice were examined. Each gene's expression was normalized to the rRNA expression level. Average values are shown, and error bars indicate standard deviations. The average values for wild-type tissues are set to 1. Representative results from two independent experiments are shown. The Student *t* test was used to calculate statistical significance (*, $P < 0.05$; **, $P < 0.01$). (C) Nuclear accumulation of Nrf2 in mice carrying floxed *Keap1* alleles. Immunoblot analysis of nuclear extracts of liver, lung, and upper digestive tract, including esophagus, forestomach, and glandular stomach, using anti-Nrf2. Eight- to 15-week old mice were examined. A representative result from two independent experiments is shown. Lamin B was detected as a loading control. Genotypes: +/+, $Keap1^{+/+}$; +/−, $Keap1^{+/-}$; F/F, $Keap1^{flox/flox}$; F/−, $Keap1^{flox/-}$; F/−:Alb, $Keap1^{flox/-}$::*Alb*-Cre; NKO, $Nrf2^{-/-}$. The band intensity of Nrf2 was quantified and normalized by the band intensity of Lamin B. The values obtained are shown below the bands of Nrf2.

pressing Cre recombinase under the regulation of the *Keratin 5* gene (*K5*-Cre mouse) to obtain $Keap1^{flox/flox}$::*K5*-Cre mice. The endogenous *K5* gene is expressed not only in skin keratinocytes but also in stratified epithelial cells of the tongue, esophagus, forestomach, cornea, and hair follicles (3).

We compared the growth, survival, and pathology of the upper digestive tract of $Keap1^{flox/flox}$::*K5*-Cre mice with those of $Keap1^{flox/flox}$, $Keap1^{flox/+}$::*K5*-Cre, and $Keap1^{flox/+}$ mice within the same litter. As we expected, $Keap1^{flox/flox}$::*K5*-Cre mice were smaller than $Keap1^{flox/+}$::*K5*-Cre and $Keap1^{flox/+}$ mice (Fig. 4A, upper panel), and the body weights of $Keap1^{flox/flox}$::*K5*-Cre mice were approximately half of those of $Keap1^{flox/flox}$, $Keap1^{flox/+}$::*K5*-Cre, and $Keap1^{flox/+}$ mice at 9 days after birth (Fig. 4B and C). Similar to the stomachs of *Keap1*-null pups (Fig. 2A), the longer diameters of $Keap1^{flox/flox}$::*K5*-Cre pup stomachs were less than half the length of the longer diameters of $Keap1^{flox/+}$ or $Keap1^{flox/+}$::*K5*-Cre pup stomachs (Fig. 4A, lower panel). The size of the $Keap1^{flox/flox}$ pup stomach was midway between the sizes of $Keap1^{flox/+}$::*K5*-Cre and $Keap1^{flox/flox}$::*K5*-Cre pup stomachs. All $Keap1^{flox/flox}$::*K5*-Cre

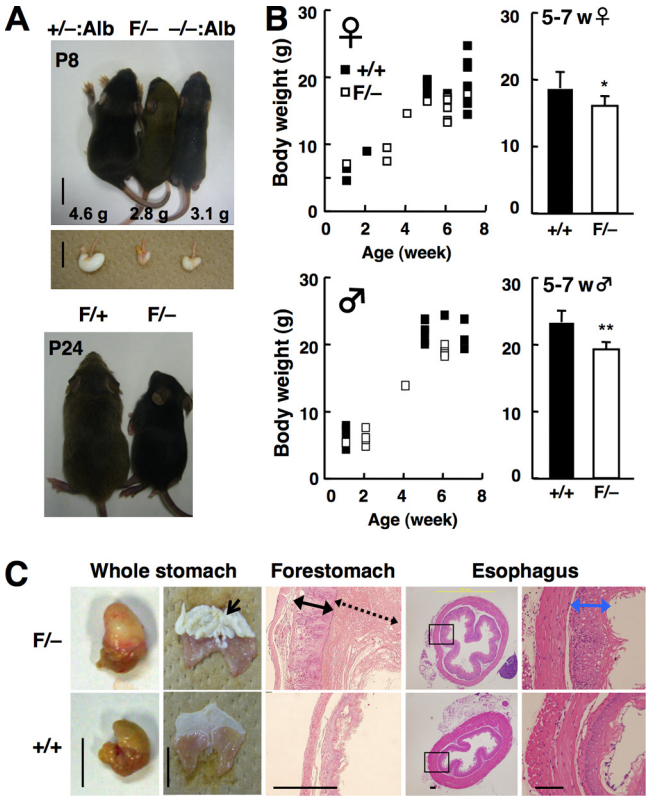

FIG. 2. Morphological alterations in upper digestive tracts of mice carrying floxed *Keap1* alleles. (A) Macroscopic observations of 8-day-old (P8) and 24-day-old (P24) male littermates. Body weights and dissected stomachs with esophagi of the 8-day-old pups are shown. White color of the stomach indicates the presence of ingested milk. Scale bars indicate 1 cm. (B) Body weight gain during weeks 1 to 8 after birth of female (upper left) and male (lower left) mice and average body weight at the age of 5 to 7 weeks of female (upper right) and male (lower right) mice. Error bars indicate standard deviations (*Keap1*$^{+/+}$ mice, $n = 18$ female and $n = 11$ male; *Keap1*$^{flox/-}$ mice, $n = 8$ female and $n = 5$ male). The Student t test was used to calculate statistical significance (*, $P < 0.05$; **, $P < 0.01$). (C) Upper digestive tracts from 9- to 13-week-old male mice. Macroscopic observation of the whole stomach and hematoxylin-eosin staining of the forestomach and esophagus are shown. Arrow, hyperkeratotic inner surface of the forestomach; double-ended arrow, hypertrophic subcornified layer; double-ended broken arrow, thickened cornified layer; double-ended blue arrow, hyperkeratotic esophageal epithelium. Vertical and horizontal scale bars indicate 1 cm and 100 μm, respectively. Genotypes: +/−:Alb, *Keap1*$^{+/-}$::*Alb*-Cre; F/−, *Keap1*$^{flox/-}$; −/−:Alb, *Keap1*$^{-/-}$::*Alb*-Cre; F/+, *Keap1*$^{flox/+}$; +/+, *Keap1*$^{+/+}$.

mice died by 14 days after birth (Fig. 4D), and this timing was quite consistent with that seen in *Keap1*-null mice (43). These results support the notion that *Keap1*-null mouse lethality is a feeding problem due to severe hyperkeratotic lesions in the upper digestive tract.

Indeed, in histological analysis of the tissues expressing K5, i.e., forestomach, esophagus, and tongue, marked thickening of cornified and subcornified layers was observed in *Keap1*$^{flox/flox}$::*K5*-Cre mice and *Keap1*$^{flox/flox}$ mice in comparison with these layers in *Keap1*$^{flox/+}$ mice (Fig. 4F, upper panels). The epithelial thickening was much more severe in *Keap1*$^{flox/flox}$::*K5*-Cre mice than in *Keap1*$^{flox/flox}$ mice.

To examine whether this graded severity of epithelial phenotypes correlates to the increase of Nrf2 activity, we examined Nrf2 accumulation in keratinocytes of these tissues by immunohistochemistry using anti-Nrf2 antibody. We found positive staining in the nuclei of *Keap1*$^{flox/flox}$ and *Keap1*$^{flox/flox}$::*K5*-Cre mouse keratinocytes but not in the keratinocyte nuclei of *Keap1*$^{flox/+}$ mice (Fig. 4F, lower panels). We repeated the analysis and found that the intensity of the immunoreactivity was consistently higher in *Keap1*$^{flox/flox}$::*K5*-Cre mice than in *Keap1*$^{flox/flox}$ mice, supporting our contention that the more Nrf2 accumulates in keratinocytes, the more severe the epithelial thickening that occurs.

To further corroborate the correlation between the Nrf2 accumulation and epithelial thickening, we examined the epidermal expression of Nrf2 target genes in these mice. The expression of canonical Nrf2 target genes, *Nqo1* and *Gpx2*, was elevated in the epidermis of *Keap1*$^{flox/flox}$ and *Keap1*$^{flox/flox}$::*K5*-Cre embryos at E18.5 (Fig. 4E). Compared with the increase in the expression of these genes in the *Keap1*$^{flox/flox}$ epidermis, the increase in their expression in the *Keap1*$^{flox/flox}$::*K5*-Cre epidermis was much more dramatic. The expression levels of *Nqo1* and *Gpx2* in the *Keap1*$^{flox/flox}$::*K5*-Cre epidermis are 23-fold and 17-fold higher than those in the *Keap1*$^{flox/flox}$ epidermis, respectively. Thus, this gene expression analysis showed that *Keap1*$^{flox/flox}$::*K5*-Cre mice displayed the highest expression of Nrf2 target genes among the genotypes examined.

Considering the fact that simultaneous deletion of Nrf2 rescued *Keap1*-null mice from developing hyperkeratotic lesions and lethality at the weaning stage, these results strongly argue that Nrf2 activation in keratinocytes is the ultimate cause of the lethality of *Keap1*-null mice. The results also suggest that Keap1 produced from the floxed *Keap1* allele in keratinocytes can direct Nrf2 degradation to such an extent that *Keap1*$^{flox/flox}$ and *Keap1*$^{flox/-}$ mice escape from the juvenile lethality.

The *Keap1* deletion in hepatocytes increases expression levels of Nrf2 target genes. We next examined the contribution of Keap1 expressed from the floxed allele to the repression of Nrf2 activity in the liver. In our previous study, we performed hepatocyte-specific disruption of the *Keap1* gene by using *Keap1*$^{flox/-}$ mice and *Alb*-Cre mice (31). We compared the knockdown mice with the hepatocyte-specific conditional knockout mice, as well as with the control wild-type mice. Although a difference in the amount of Nrf2 nuclear accumulation was not apparent between *Keap1*$^{flox/-}$ and *Keap1*$^{flox/-}$::*Alb*-Cre mice (Fig. 1C), the expression levels of some Nrf2 target genes, such as *Gclc*, *Gsta4*, and *Gstp2*, were higher in *Keap1*$^{flox/-}$::*Alb*-Cre mouse livers than in *Keap1*$^{flox/-}$ mouse livers (Fig. 5, right panels). In contrast, the expression levels of other Nrf2 target genes, such as *Ho-1*, *Gpx1* and *Gstp1*, were not changed significantly in the livers of *Keap1*$^{flox/-}$ mice and *Keap1*$^{flox/-}$::*Alb*-Cre mice compared to their levels in wild-type mouse livers (Fig. 5, left panels). These results thus indicate that Keap1 expressed from the floxed allele contributes substantially to the repression of a set of Nrf2 target genes in the liver. These results further suggest that Nrf2 target genes are under complex regulation and that each of them retains a distinct threshold for the amount of Nrf2 required for activation. Subtle changes in the Nrf2 abundance in nuclei thus appear to make specific contributions to target gene expression. Furthermore, recent reports on Keap1-interacting molecules (6, 22, 24) suggest possible

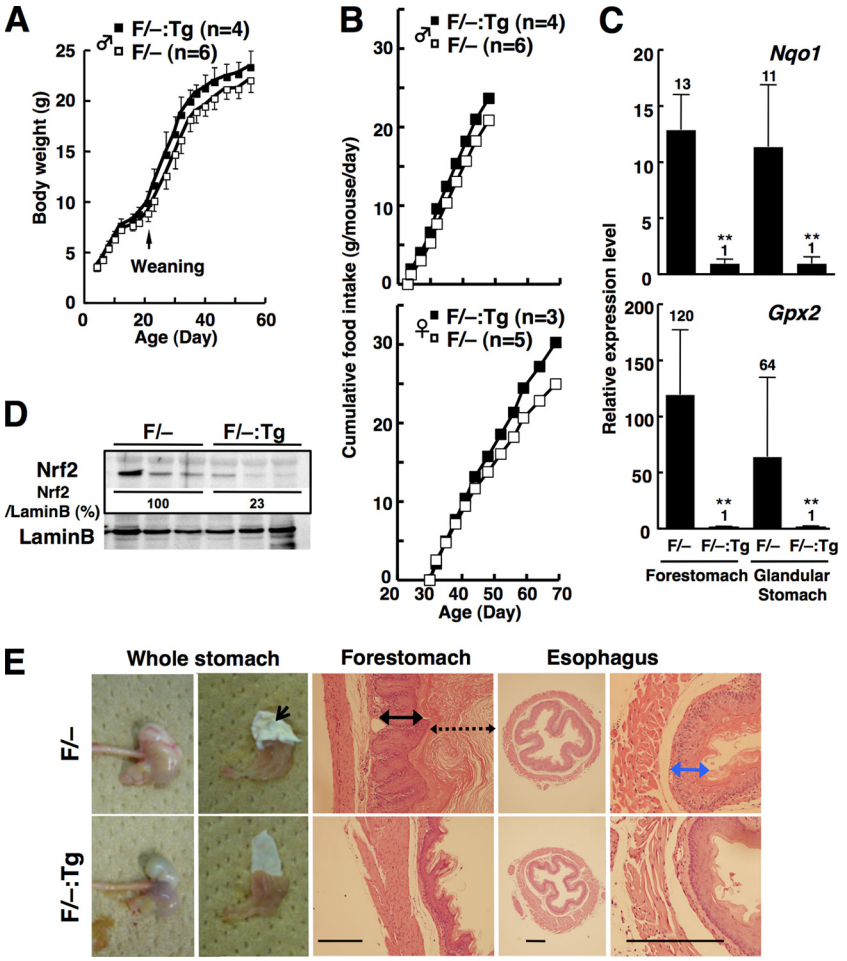

FIG. 3. Rescue of the *Keap1* knockdown phenotypes by transgene (Tg)-derived Keap1 (*KRD*-Keap1). (A to C) Graphs show body weights (A), cumulative food intake (B), and *Nqo1* and *Gpx2* mRNA expression levels in forestomach and glandular stomach (C) of 8-week-old male littermates. Each gene's expression was normalized to the rRNA expression level. Average values are shown, and error bars indicate standard deviations (*Keap1*$^{flox/-}$ mice, $n = 6$; *Keap1*$^{flox/-}$::*KRD*-Keap1 mice, $n = 4$). The Student t test was used to calculate statistical significance (**, $P < 0.01$). (D) Immunoblot analysis of Nrf2 using liver extracts. Lamin B was detected as a loading control. The band intensity of Nrf2 was quantified and normalized to the band intensity of Lamin B. Average values of the triplicate samples are shown below the bands of Nrf2. (E) Morphology of upper digestive tract. Macroscopic observations of whole stomach and hematoxylin-eosin staining of forestomach and esophagus are shown. Arrow, hyperkeratotic inner surface of the forestomach; double-ended arrow, hypertrophic subcornified layer; double-ended broken arrow, thickened cornified layer; double-ended blue arrow, hyperkeratotic esophageal epithelium. Scale bars indicate 200 μm. Genotypes: F/−, *Keap1*$^{flox/-}$; F/−:Tg, *Keap1*$^{flox/-}$::*KRD*-Keap1.

contributions of these factors to the expression of Nrf2 target genes in the liver.

Decreased Keap1 confers resistance against acute toxicity of APAP. It has been shown that Nrf2 is protective against APAP toxicity and that *Nrf2*-null mice are more susceptible to acute hepatotoxicity of APAP (9). Nrf2 regulates a series of enzymes responsible for detoxification of APAP (10, 19, 23, 27, 37, 40), including *Ugts*, *Gsts*, and *Mrps*. The *Gclc* gene encodes a component of the rate-limiting enzyme for glutathione production, GCL, and is also under the regulation of Nrf2. We previously challenged *Keap1*$^{flox/-}$::*Alb*-Cre mice with a high dose of APAP and found that *Keap1*$^{flox/-}$::*Alb*-Cre mice were more resistant to APAP toxicity than *Keap1*$^{+/+}$::*Alb*-Cre mice (31).

Because we found in this study that *Gclc* expression is elevated in *Keap1*$^{flox/-}$ mice (Fig. 5), we challenged *Keap1*$^{flox/-}$ mice with APAP, expecting that *Keap1*$^{flox/-}$ mice would also be resistant to the APAP acute toxicity. We compared the survival of *Keap1*$^{flox/-}$ mice after the administration of APAP with that of *Keap1*$^{flox/-}$::*Alb*-Cre, *Keap1*$^{flox/+}$::*Alb*-Cre, and wild-type mice. As shown in Fig. 6A, a sublethal dose of APAP (700 mg/kg) was administered to mice of the four different genotypes, and their survival was followed up to 48 h. Consistent with the results of our previous study, wild-type mice were the most susceptible to APAP toxicity, and almost half of the mice died by 48 h. In contrast, *Keap1*$^{flox/-}$::*Alb*-Cre mice showed resistance to the APAP challenge.

To our surprise, *Keap1*$^{flox/-}$ mice and *Keap1*$^{flox/+}$::*Alb*-Cre mice were more resistant to APAP than *Keap1*$^{flox/-}$::*Alb*-Cre mice. After the APAP injection, low body temperature, tremor, sedation, and lethargy were observed irrespective of the genotype. Closer examination revealed that *Keap1*$^{flox/-}$ mice not only had a lower mortality rate but also recovered more quickly from these

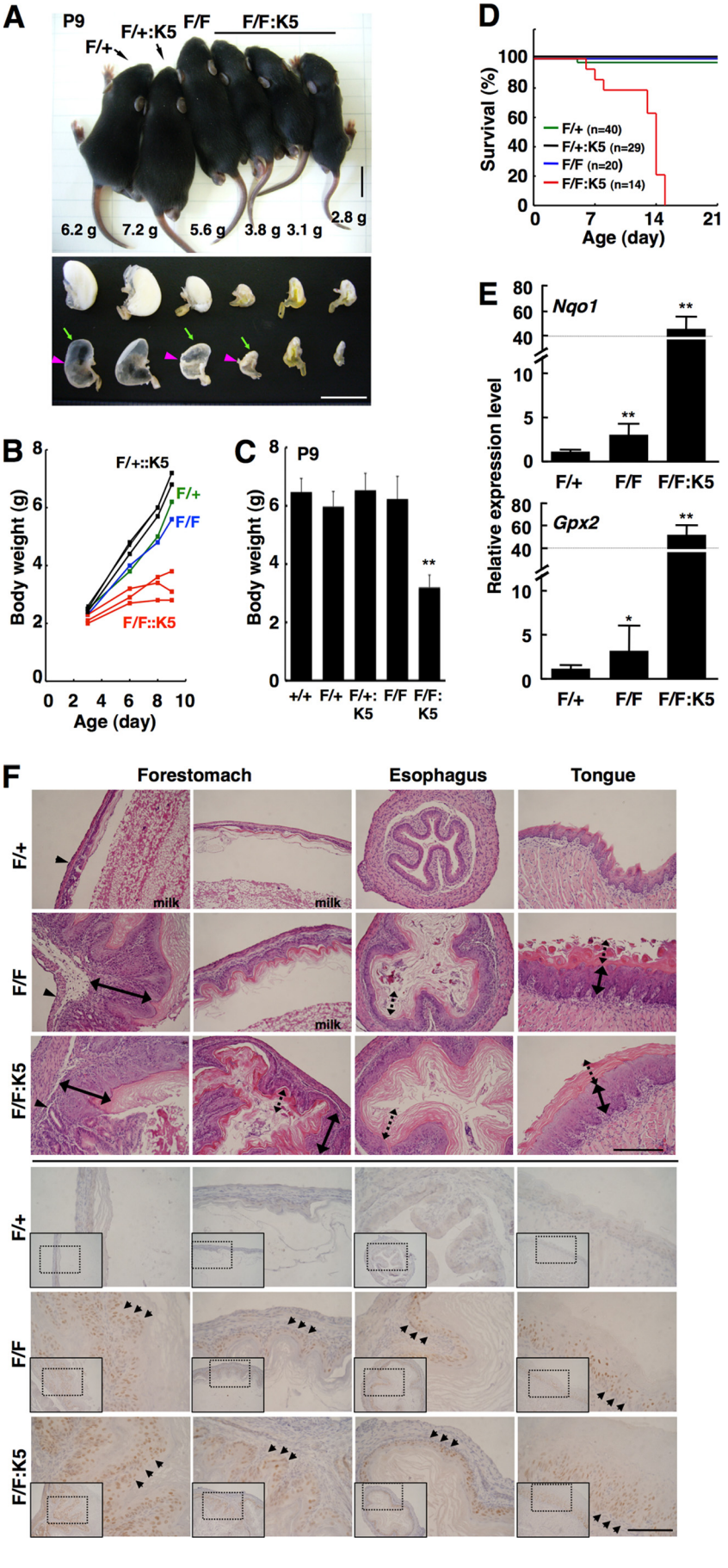
A
P9
F/+
F/+:K5
F/F
F/F:K5
6.2 g
7.2 g
5.6 g
3.8 g
3.1 g
2.8 g
B
F/+::K5
F/+
F/F
F/F::K5
Body weight (g)
Age (day)
C
P9
Body weight (g)
+/+
F/+
F/+: K5
F/F
F/F: K5
D
Survival (%)
F/+ (n=40)
F/+:K5 (n=29)
F/F (n=20)
F/F:K5 (n=14)
Age (day)
E
Nqo1
Gpx2
Relative expression level
F/+
F/F
F/F:K5
F
Forestomach
Esophagus
Tongue
milk

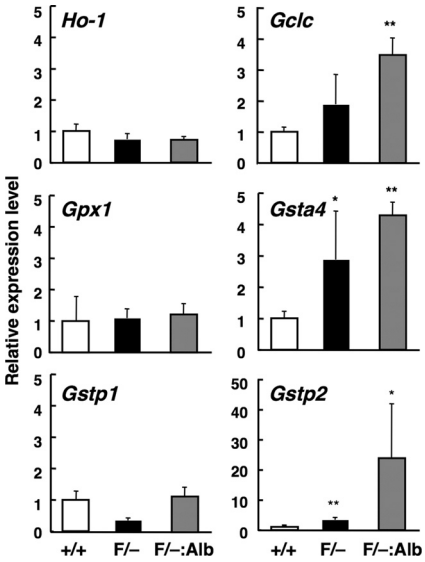

FIG. 5. Expression of Nrf2 target genes in the livers of mice carrying floxed *Keap1* alleles. Ten- to 12-week-old female mice were examined. Average values are shown, and error bars indicate standard deviations. Each gene's expression was normalized to the rRNA expression level. The average values for wild-type mice are set to 1. The Student *t* test was used to calculate statistical significance (*, $P < 0.05$; **, $P < 0.01$). Genotypes: +/+, *Keap1*$^{+/+}$; F/−, *Keap1*$^{flox/-}$; F/−:Alb, *Keap1*$^{flox/-}$::*Alb*-Cre.

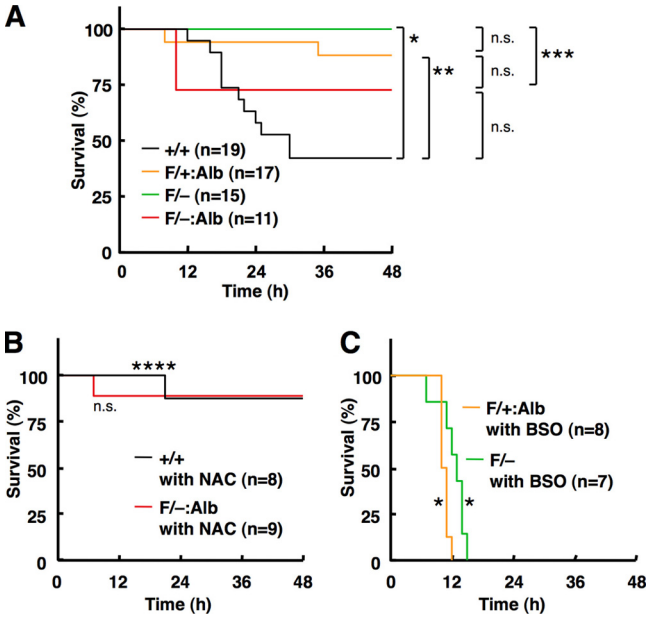

FIG. 6. Kaplan-Meier survival curves for mice treated with APAP. Seven- to 10-week old female mice carrying floxed *Keap1* alleles were intraperitoneally injected with APAP (A), APAP and NAC (B), and APAP and BSO (C). Mortality was measured over a 48-hour period. The log rank test was used to calculate statistical significance (*, $P < 0.001$; **, $P < 0.01$; ***, $P < 0.05$; ****, $P < 0.1$; n.s., not significant). *P* values in panels B and C were calculated against the results for mice of the same genotype that were given APAP only (A). Genotypes: +/+, *Keap1*$^{+/+}$; F/+:Alb, *Keap1*$^{flox/+}$::*Alb*-Cre; F/−, *Keap1*$^{flox/-}$; F/−:Alb, *Keap1*$^{flox/-}$::*Alb*-Cre.

conditions. These results thus demonstrate that reduced expression of Keap1 is beneficial for hepatocytes to acquire resistance to APAP toxicity and that the complete loss of Keap1 is not optimal for the protection of the hepatocytes.

Concomitant administration of NAC, a precursor to glutathione, was protective for *Keap1*$^{flox/-}$::*Alb*-Cre and wild-type mice (Fig. 6B). On the contrary, simultaneous administration of BSO, an inhibitor of GCL, sensitized *Keap1*$^{flox/-}$ and *Keap1*$^{flox/+}$::*Alb*-Cre mice (Fig. 6C). These results support our contention that the availability of glutathione determines the susceptibility to APAP toxicity. Therefore, enhanced Nrf2 activity may be advantageous for the protection of liver function and the survival of the mice, probably through increasing the capacity for glutathione production.

Decrease of Keap1 expression is not beneficial for the long-term survival of mice. We finally examined how changes in the Keap1 expression level influence the long-term survival of mice. In our long-term follow-up study, *Keap1*$^{flox/-}$ and *Keap1*$^{flox/-}$::*Alb*-Cre mice remained as healthy as *Keap1*$^{flox/+}$::*Alb*-Cre and wild-type mice for up to 1 year (Fig. 7A). However, after the 1-year time point, significant numbers of *Keap1*$^{flox/-}$ and *Keap1*$^{flox/-}$::*Alb*-Cre mice started to die. By 2 years, close to 50% of *Keap1*$^{flox/-}$::*Alb*-Cre and more than 50% of *Keap1*$^{flox/-}$ mice were dead, while more than 70% of *Keap1*$^{flox/+}$::*Alb*-Cre and wild-type mice stayed alive. There was no statistically significant gender difference in the long-term survival rates.

At 1 year of age, *Keap1*$^{flox/-}$ and *Keap1*$^{flox/-}$::*Alb*-Cre mice appeared to be smaller in size than *Keap1*$^{flox/+}$::*Alb*-Cre and wild-type mice (data not shown). The average body weights at 1.6 to 1.7 years of age were clearly lower in *Keap1*$^{flox/-}$ (16.0 ± 2.0 g) and *Keap1*$^{flox/-}$::*Alb*-Cre (20.2 ± 5.0 g) mice than in

FIG. 4. Keratinocyte-specific *Keap1* knockout mice using *K5*-Cre. (A) Macroscopic appearance of 9-day-old (P9) littermates. Body weights and whole stomachs are shown at the bottom. Scale bars indicate 1 cm. (B) Body weight gain during the period from day 3 to day 9. (C) Body weights at day 9 (P9). The average and standard deviation were calculated, and the Student *t* test was used to calculate statistical significance compared with results for *Keap1*$^{flox/+}$ mice (**, $P < 0.01$). (D) Kaplan-Meier survival curve. (E) Expression of Nrf2 target genes in keratinocytes at E18.5. Each gene's expression was normalized to the level of rRNA expression. Average values are shown, and error bars indicate standard deviations. The average values of wild-type samples are set to 1. The Student *t* test was used to calculate statistical significance (*, $P < 0.05$; **, $P < 0.01$). (F) Hematoxylin-eosin staining (upper panels) and immunohistochemical staining with anti-Nrf2 antibody (lower panels) of the forestomach, esophagus, and tongue. The positions shown in the left and right panel images from the forestomach are indicated by arrowheads and arrows, respectively, in panel A. Symbols in upper panels: arrowheads, limiting ridge; double-ended arrows, hypertrophic subcornified layer; double-ended broken arrows, thickened cornified layer. Arrowheads in lower panels indicate representative nuclei of keratinocytes that show positive staining. The areas shown in the lower panels correspond to dotted rectangles in the inset views, which are at a lower magnification. Scale bars indicate 200 μm (upper panels) and 400 μm (lower panels). Genotypes: F/+, *Keap1*$^{flox/+}$; F/+:K5, *Keap1*$^{flox/+}$::*K5*-Cre; F/F, *Keap1*$^{flox/flox}$; F/F:K5, *Keap1*$^{flox/flox}$::*K5*-Cre; +/+, *Keap1*$^{+/+}$.

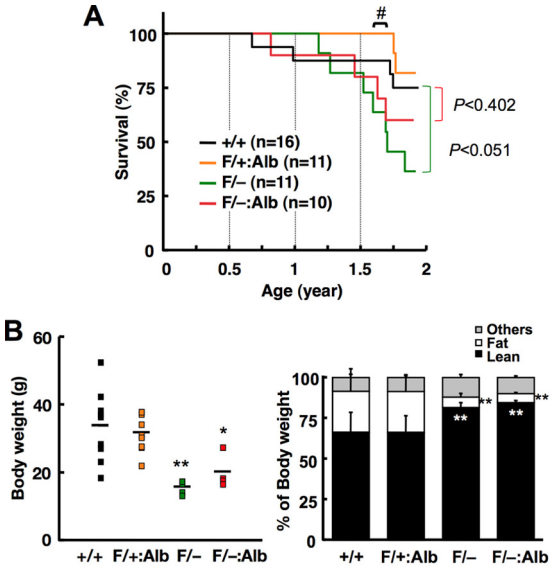

FIG. 7. Longevity study of mice carrying floxed *Keap1* alleles. (A) Kaplan-Meier survival curves for female mice are shown. Mortality was measured over a 2-year period (101 weeks). $Keap1^{+/+}$ ($n = 16$), $Keap1^{flox/+}$::*Alb*-Cre ($n = 11$), $Keap1^{flox/-}$ ($n = 11$), and $Keap1^{flox/-}$::*Alb*-Cre ($n = 10$) mice were examined. The log rank test was used to calculate statistical significance. (B) Body weight and body composition of lean and fat are shown. Female mice at 1.6 to 1.7 years of age (the starting number in each group is shown in panel A) with the $Keap1^{+/+}$ ($n = 9$), $Keap1^{flox/+}$::*Alb*-Cre ($n = 10$), $Keap1^{flox/-}$ ($n = 5$) and $Keap1^{flox/-}$::*Alb*-Cre ($n = 4$) genotypes that survived were examined. Bar graph shows the average ratios of lean, fat, and other body compositions, and standard deviations are indicated. The Student *t* test was used to calculate statistical significance compared with the results for $Keap1^{+/+}$ mice. *, $P < 0.05$; **, $P < 0.01$. Genotypes: +/+, $Keap1^{+/+}$; F/+:Alb, $Keap1^{flox/+}$::*Alb*-Cre; F/−, $Keap1^{flox/-}$; F/−:Alb, $Keap1^{flox/-}$::*Alb*-Cre.

$Keap1^{flox/+}$::*Alb*-Cre (31.8 ± 5.2 g) and wild-type (34.0 ± 10.5 g) mice (Fig. 7B, left panel). We also measured body composition and found that $Keap1^{flox/-}$ and $Keap1^{flox/-}$::*Alb*-Cre mice retained body compositions that were strikingly different from those of $Keap1^{flox/+}$::*Alb*-Cre and wild-type mice. The ratios of fat and lean of the former are significantly lower and higher than those of the latter, respectively (Fig. 7B, right panel). These results demonstrate that systemic and genetic reduction of Keap1 to a level less than a certain threshold gives rise to the limitation of the life span accompanied by leanness and imply that constitutive activation of Nrf2 over a long period is not beneficial to the animal's survival.

DISCUSSION

In the present study, we discovered that floxation of the *Keap1* allele using *loxP* sites in the design of a conditional *Keap1*-null mouse led to a partial disruption of Keap1 expression, which created a whole-body knockdown phenotype that escaped from early lethality but exhibited many characteristics similar to those of the *Keap1*-null mice. Through analyses of the mice possessing the floxed allele of the *Keap1* gene, we found that the chronic and whole-body activation of Nrf2 due to insufficiency of Keap1 function is beneficial during acute insults from chemical toxicity, which is consistent with the well-established notion that inducible expression of cytoprotective enzymes by transiently activated Nrf2 is important for protection of the body (17). In contrast, the sustained systemic activation of Nrf2 turned out to be rather disadvantageous for long-term survival of the mice. Being viable and fertile, the *Keap1* gene knockdown mice provided a useful experimental system for the study of Keap1 function in adult mice.

We speculate that the insertion of the EGFP cassette into the 3′ region of the *Keap1* gene (31) somehow disrupted critical regulatory elements for transcription of the *Keap1* gene. Consequently, Keap1 expression was decreased in various tissues of the $Keap1^{flox/flox}$ and $Keap1^{flox/-}$ mice, and they had phenotypes similar to those of *Keap1*-null mice (43). However, these knockdown mice can escape from the juvenile lethality. These phenotypic changes in the $Keap1^{flox/-}$ mice are directly due to a decrease in Keap1 expression, because transgene-derived Keap1 restored the abnormalities in $Keap1^{flox/-}$ mice. We further performed keratinocyte-specific deletion of the *Keap1* gene using *K5*-Cre mice and found that the keratinocyte-specific *Keap1* deletion resulted in the dramatic activation of Nrf2 target genes and lethality at the weaning age. These results conclusively demonstrate that the lethality of *Keap1*-null mice is attributable to the malnutrition caused by obstructive lesions in the upper digestive tract and that Keap1 deficiency in the keratinocytes is the primary cause of the *Keap1*-null mouse lethality.

Utilizing the floxed *Keap1* allele, a series of mice with graded expression levels of the *Keap1* gene become available. These mice enabled us to perform the titration of Keap1 abundance *in vivo*, especially in hepatocytes, to clarify how the graded and constitutive activation of Nrf2 affects the animal's life and homeostasis. Since the amount of Keap1 produced from the floxed allele is estimated as approximately 5% of that from the wild-type allele (Fig. 1A), $Keap1^{flox/+}$::*Alb*-Cre mice (along with $Keap1^{+/-}$ mice), $Keap1^{flox/-}$ mice, and $Keap1^{flox/-}$::*Alb*-Cre mouse hepatocytes contain 50%, 5%, and 0% of the amount of Keap1 in wild-type mouse hepatocytes, respectively. Treatment of $Keap1^{flox/+}$::*Alb*-Cre, $Keap1^{flox/-}$, $Keap1^{flox/-}$::*Alb*-Cre, and wild-type mice with 700 mg/kg APAP revealed that constitutive activation of Nrf2 is beneficial during acute toxicity, which is consistent with the results of our previous study (31).

An unexpected but intriguing result is that $Keap1^{flox/+}$::*Alb*-Cre and $Keap1^{flox/-}$ mice show stronger resistance to APAP than the $Keap1^{flox/-}$::*Alb*-Cre mice, suggesting that the maximal benefit of Nrf2 activation is given by a level of Keap1 somewhere between a 50% ($Keap1^{flox/+}$::*Alb*-Cre mice) and a 5% level ($Keap1^{flox/-}$ mice), but the complete loss of Keap1 in $Keap1^{flox/-}$::*Alb*-Cre mice appears to be less beneficial. In this regard, we recently found sporadic focal necrosis in livers of $Keap1^{flox/-}$::*Alb*-Cre mice, indicating that some of the $Keap1^{flox/-}$::*Alb*-Cre mice suffered from hepatitis (22). We speculate that the $Keap1^{flox/-}$::*Alb*-Cre mice with hepatitis are vulnerable to APAP toxicity, which could lower the survival ratio of the $Keap1^{flox/-}$::*Alb*-Cre mice. In terms of Nrf2 activity, these results just fit a "U-shaped dose-response curve" model that has been proposed recently (17). Either deficiency or constitutive activation of Nrf2 increases the risk of carcinogenesis, and there is a certain optimal range of Nrf2 activity for the most efficient cancer prevention. Similarly, for increasing resistance against APAP toxicity, there is an optimal level of Nrf2

activity that must be attained in *Keap1*$^{flox/+}$::*Alb*-Cre mice and *Keap1*$^{flox/-}$ mice.

We found that the concomitant administration of BSO or NAC gave rise to exacerbation of or increased resistance to APAP toxicity, respectively. This observation provides convincing evidence that the availability of glutathione is an important determinant of resistance/susceptibility to APAP toxicity. Whereas *Gclc* gene expression is upregulated in the *Keap1*$^{flox/-}$ mouse liver, the amount of total hepatic glutathione remained constant (K. Taguchi and M. Yamamoto, unpublished observations). In contrast, total glutathione levels in the upper digestive tract of *Keap1*$^{flox/-}$ mice were approximately 3-fold higher, in accordance with the upregulation of *Gclc* mRNA and protein levels (K. Taguchi and M. Yamamoto, unpublished observations). As the hepatic glutathione level is far higher than that in other tissues, total hepatic glutathione may be regulated by feedback autoinhibition by glutathione or by the limited availability of cellular L-cysteine (25). Since Nrf2 activates a battery of genes involved in reducing oxidized glutathione, such as glutathione reductase and glucose 6-phosphate dehydrogenase (40), the ratio of reduced glutathione could be higher in the livers of *Keap1*$^{flox/-}$ mice, and this might confer resistance against APAP toxicity.

Besides inhibiting GCL, BSO accelerates Cyp2e1-dependent metabolism (8). Cyp2e1 oxidizes acetaminophen to its active metabolite, *N*-acetyl-*p*-benzoquinoneimine, which is cytotoxic due to DNA and protein adduct formation. Thus, the emerging toxicity of APAP when coadministered with BSO in *Keap1*$^{flox/-}$ mice and *Keap1*$^{flox/+}$::*Alb*-Cre mice, which were otherwise resistant to APAP, might be attributable to not only glutathione depletion but also facilitated metabolism of APAP due to increased activity of Cyp2e1.

When examined in a 2-year longevity study, *Keap1*$^{flox/-}$ and *Keap1*$^{flox/-}$::*Alb*-Cre mice showed higher mortality rates than *Keap1*$^{flox/+}$::*Alb*-Cre and wild-type mice. This analysis demonstrates that genetic disruption of *Keap1* gene expression by more than 50% provokes the Nrf2 activation to a level that has a negative impact on long-term survival of the mice. This is in stark contrast to the fact that pharmacological induction of Nrf2 by antioxidants and electrophiles prevents acute toxicity of APAP and other chemicals. We surmise that the genetic activation of Nrf2 may lead to high-level constitutive activation of the genes that are usually associated with the stress response in the normal physiological context but may not contribute to the protection of the whole body. These observations further support the importance of inducible/transient expression of cytoprotective enzymes in the body (17). To further consolidate our notion that high-level constitutive activation of Nrf2 target genes is not truly beneficial to the whole body, long-term survival studies of *Keap1*::*Nrf2* double mutant mice seem to be crucial.

After one and a half years of age, the body weights and body compositions of *Keap1*$^{flox/-}$ and *Keap1*$^{flox/-}$::*Alb*-Cre mice are low and lean, respectively, compared to those of *Keap1*$^{flox/+}$::*Alb*-Cre and wild-type mice. The reduction in body weight and fat ratio might be caused by either decreased food intake or increased energy expenditure. The former cause would be plausible as hyperkeratotic lesions are present in the upper digestive tracts of *Keap1*$^{flox/-}$ and *Keap1*$^{flox/-}$::*Alb*-Cre mice, and this limits the amount of food intake. The latter would also be possible since Nrf2 strongly activates cytoprotective gene expression, resulting in the robust increase of protein synthesis. Chronic activation of Nrf2 could increase the anabolic energy demand. A recent report demonstrated that Nrf2 inhibits adipogenesis through induction of the arylhydrocarbon receptor (35). Further elucidation of the Nrf2 contribution to metabolism is an important challenge.

Another important result obtained from the 2-year longevity study is that neither *Keap1*$^{flox/-}$ nor *Keap1*$^{flox/-}$::*Alb*-Cre mice developed tumors. Although Nrf2 itself has been shown to be a critical component of cancer chemoprevention (2, 33), recent studies have also revealed a strong association of constitutive activation of Nrf2 due to somatic mutations of *KEAP1* and the *NRF2* gene and carcinogenesis (30, 32, 34, 36). Cancer cells harboring constitutive Nrf2 accumulation are resistant to chemotherapy owing to the high-level expression of efflux transporters and antioxidative and detoxifying enzymes (30, 34, 36). Indeed, the upper digestive tracts of both *Keap1*$^{flox/-}$ and *Keap1*$^{flox/-}$::*Alb*-Cre mice display keratin swirl, epithelial cornification, and cellular morphological changes that resemble epithelial dysplasia. However, in our present study, these lesions never developed into genuine cancers, suggesting that the activation of Nrf2 is not solely sufficient to facilitate cell transformation into malignancy. It is strongly suspected that Nrf2 confers a high survival capacity only after cells acquire the ability of immortalized growth.

ACKNOWLEDGMENTS

We thank Naomi Kaneko, Martin J. Pfeiffer, Eriko Naganuma, and the Biomedical Research Core of Tohoku University Graduate School of Medicine for technical support and Junji Takeda (Osaka University) for kindly providing *K5*-Cre transgenic mice.

This work was supported in part by Grants-in-Aids for Creative Scientific Research, Scientific Research on Priority Areas, and Scientific Research from JSPS, as well as by the Target Protein Program from MEXT, by Tohoku University's Global COE Program (funded by JSPS) for Conquest of Signal Transduction Diseases with Network Medicine, and by ERATO funding from JST.

REFERENCES

1. **Aoki, Y., H. Sato, N. Nishimura, S. Takahashi, K. Itoh, and M. Yamamoto.** 2001. Accelerated DNA adduct formation in the lung of the Nrf2 knockout mouse exposed to diesel exhaust. Toxicol. Appl. Pharmacol. **173:**154–160.
2. **auf dem Keller, U., M. Huber, T. A. Beyer, A. Kümin, C. Siemes, S. Braun, P. Bugnon, V. Mitropoulos, D. A. Johnson, J. A. Johnson, D. Hohl, and S. Werner.** 2006. Nrf transcription factors in keratinocytes are essential for skin tumor prevention but not for wound healing. Mol. Cell. Biol. **26:**3773–3784.
3. **Byrne, C., and E. Fuchs.** 1993. Probing keratinocyte and differentiation specificity of the human K5 promoter in vitro and in transgenic mice. Mol. Cell. Biol. **3:**3176–3190.
4. **Chan, K., R. Lu, J. C. Chang, and Y. W. Kan.** 1996. NRF2, a member of the NFE2 family of transcription factors, is not essential for murine erythropoiesis, growth, and development. Proc. Natl. Acad. Sci. U. S. A. **93:**13943–13948.
5. **Chan, K., X. D. Han, and Y. W. Kan.** 2001. An important function of Nrf2 in combating oxidative stress: detoxification of acetaminophen. Proc. Natl. Acad. Sci. U. S. A. **98:**4611–4616.
6. **Chen, W., Z. Sun, X. J. Wang, T. Jiang, Z. Huang, D. Fang, and D. D. Zhang.** 2009. Direct interaction between Nrf2 and p21(Cip1/WAF1) upregulates the Nrf2-mediated antioxidant response. Mol. Cell **34:**663–673.
7. **Dinkova-Kostova, A. T., W. D. Holtzclaw, R. N. Cole, K. Itoh, N. Wakabayashi, Y. Katoh, M. Yamamoto, and P. Talalay.** 2002. Direct evidence that sulfhydryl groups of Keap1 are the sensors regulating induction of phase 2 enzymes that protect against carcinogens and oxidants. Proc. Natl. Acad. Sci. U. S. A. **99:**11908–11913.
8. **Donohue, T. M., Jr., T. V. Curry-McCoy, S. L. Todero, R. L. White, K. K. Kharbanda, A. A. Nanji, and N. A. Osna.** 2007. L-Buthionine (S,R) sulfoximine depletes hepatic glutathione but protects against ethanol-induced liver injury. Alcohol. Clin. Exp. Res. **31:**1053–1060.

9. **Enomoto, A., K. Itoh, E. Nagayoshi, J. Haruta, T. Kimura, T. O'Connor, T. Harada, and M. Yamamoto.** 2001. High sensitivity of Nrf2 knockout mice to acetaminophen hepatotoxicity associated with decreased expression of ARE-regulated drug metabolizing enzymes and antioxidant genes. Toxicol. Sci. **59:**169–177.
10. **Hayashi, A., H. Suzuki, K. Itoh, M. Yamamoto, and Y. Sugiyama.** 2003. Transcription factor Nrf2 is required for the constitutive and inducible expression of multidrug resistance-associated protein 1 in mouse embryo fibroblasts. Biochem. Biophys. Res. Commun. **310:**824–829.
11. **Hong, F., K. R. Sekhar, M. L. Freeman, and D. C. Liebler.** 2005. Specific patterns of electrophile adduction trigger Keap1 ubiquitination and Nrf2 activation. J. Biol. Chem. **280:**31768–31775.
12. **Hong, F., M. L. Freeman, and D. C. Liebler.** 2005. Identification of sensor cysteines in human Keap1 modified by the cancer chemopreventive agent sulforaphane. Chem. Res. Toxicol. **18:**1917–1926.
13. **Iizuka, T., Y. Ishii, K. Itoh, T. Kiwamoto, T. Kimura, Y. Matsuno, Y. Morishima, A. E. Hegab, S. Homma, A. Nomura, T. Sakamoto, M. Shimura, A. Yoshida, M. Yamamoto, and K. Sekizawa.** 2005. Nrf2-deficient mice are highly susceptible to cigarette smoke-induced emphysema. Genes Cells **10:** 1113–1125.
14. **Itoh, K., T. Chiba, S. Takahashi, T. Ishii, K. Igarashi, Y. Katoh, T. Oyake, N. Hayashi, K. Satoh, I. Hatayama, M. Yamamoto, and Y. Nabeshima.** 1997. An Nrf2/small Maf heterodimer mediates the induction of phase II detoxifying enzyme genes through antioxidant response elements. Biochem. Biophys. Res. Commun. **236:**313–322.
15. **Itoh, K., N. Wakabayashi, Y. Katoh, T. Ishii, K. Igarashi, J. D. Engel, and M. Yamamoto.** 1999. Keap1 represses nuclear activation of antioxidant responsive elements by Nrf2 through binding to the amino-terminal Neh2 domain. Genes Dev. **13:**76–86.
16. **Katoh, Y., K. Iida, M. I. Kang, A. Kobayashi, M. Mizukami, K. I. Tong, M. McMahon, J. D. Hayes, K. Itoh, and M. Yamamoto.** 2005. Evolutionary conserved N-terminal domain of Nrf2 is essential for the Keap1-mediated degradation of the protein by proteasome. Arch. Biochem. Biophys. **433:** 342–350.
17. **Kensler, T. W., and N. Wakabayashi.** 2010. Nrf2: friend or foe for chemoprevention? Carcinogenesis **31:**90–99.
18. **Khor, T. O., M. T. Huang, K. H. Kwon, J. Y. Chan, B. S. Reddy, and A. N. Kong.** 2006. Nrf2-deficient mice have an increased susceptibility to dextran sulfate sodium-induced colitis. Cancer Res. **66:**11580–11584.
19. **Kimura, A., Y. Ishida, T. Hayashi, T. Wada, H. Yokoyama, T. Sugaya, N. Mukaida, and T. Kondo.** 2006. Interferon-gamma plays protective roles in sodium arsenite-induced renal injury by up-regulating intrarenal multidrug resistance-associated protein 1 expression. Am. J. Pathol. **169:**1118–1128.
20. **Kobayashi, A., M. I. Kang, H. Okawa, M. Ohtsuji, Y. Zenke, T. Chiba, K. Igarashi, and M. Yamamoto.** 2004. Oxidative stress sensor Keap1 functions as an adaptor for Cul3-based E3 ligase to regulate proteasomal degradation of Nrf2. Mol. Cell. Biol. **24:**7130–7139.
21. **Kobayashi, M., L. Li, N. Iwamoto, Y. Nakajima-Takagi, H. Kaneko, Y. Nakayama, M. Eguchi, Y. Wada, Y. Kumagai, and M. Yamamoto.** 2009. The antioxidant defense system Keap1-Nrf2 comprises a multiple sensing mechanism for responding to a wide range of chemical compounds. Mol. Cell. Biol. **29:**493–502.
22. **Komatsu, M., H. Kurokawa, S. Waguri, K. Taguchi, A. Kobayashi, Y. Ichimura, Y. S. Sou, I. Ueno, A. Sakamoto, K. I. Tong, M. Kim, Y. Nishito, S. Iemura, T. Natsume, T. Ueno, E. Kominami, H. Motohashi, K. Tanaka, and M. Yamamoto.** 2010. The selective autophagy substrate p62 activates the stress responsive transcription factor Nrf2 through inactivation of Keap1. Nat. Cell Biol. **12:**213–223.
23. **Kwak, M. K., N. Wakabayashi, K. Itoh, H. Motohashi, M. Yamamoto, and T. W. Kensler.** 2003. Modulation of gene expression by cancer chemopreventive dithiolethiones through the Keap1-Nrf2 pathway. Identification of novel gene clusters for cell survival. J. Biol. Chem. **278:**8135–8145.
24. **Lee, D. F., H. P. Kuo, M. Liu, C. K. Chou, W. Xia, Y. Du, J. Shen, C. T. Chen, L. Huo, M. C. Hsu, C. W. Li, Q. Ding, T. L. Liao, C. C. Lai, A. C. Lin, Y. H. Chang, S. F. Tsai, L. Y. Li, and M. C. Hung.** 2009. KEAP1 E3 ligase-mediated downregulation of NF-kappaB signaling by targeting IKKbeta. Mol. Cell **36:**131–140.
25. **Lu, S. C.** 2000. Regulation of glutathione synthesis. Curr. Top. Cell. Regul. **36:**95–116.
26. **Luo, Y., A. L. Eggler, D. Liu, G. Liu, A. D. Mesecar, and R. B. van Breemen.** 2007. Sites of alkylation of human Keap1 by natural chemoprevention agents. J. Am. Soc. Mass Spectrom. **18:**2226–2232.
27. **Maher, J. M., X. Cheng, A. L. Slitt, M. Z. Dieter, and C. D. Klaassen.** 2005. Induction of the multidrug resistance-associated protein family of transporters by chemical activators of receptor-mediated pathways in mouse liver. Drug Metab. Dispos. **33:**956–962.
28. **Maher, J. M., M. Z. Dieter, L. M. Aleksunes, A. L. Slitt, G. Guo, Y. Tanaka, G. L. Scheffer, J. Y. Chan, J. E. Manautou, Y. Chen, T. P. Dalton, M. Yamamoto, and C. D. Klaassen.** 2007. Oxidative and electrophilic stress induces multidrug resistance-associated protein transporters via the nuclear factor-E2-related factor-2 transcriptional pathway. Hepatology **46:** 1597–1610.

28a. **Maruyama, A., S. Tsukamoto, K. Nishikawa, A. Yoshida, N. Harada, K. Motojima, T. Ishii, A. Nakane, M. Yamamoto, and K. Itoh.** 2008. Nrf2 regulates the alternative first exons of CD36 in macrophages through specific antioxidant response elements. Arch. Biochem. Biophys. **477:**139–145.

29. **Motohashi, H., and M. Yamamoto.** 2004. Nrf2-Keap1 defines a physiologically important stress response mechanism. Trends Mol. Med. **10:**549–557.
30. **Ohta, T., K. Iijima, M. Miyamoto, I. Nakahara, H. Tanaka, M. Ohtsuji, T. Suzuki, A. Kobayashi, J. Yokota, T. Sakiyama, T. Shibata, M. Yamamoto, and S. Hirohashi.** 2008. Loss of Keap1 function activates Nrf2 and provides advantages for lung cancer cell growth. Cancer Res. **68:**1303–1309.
31. **Okawa, H., H. Motohashi, A. Kobayashi, H. Aburatani, T. W. Kensler, and M. Yamamoto.** 2006. Hepatocyte-specific deletion of the keap1 gene activates Nrf2 and confers potent resistance against acute drug toxicity. Biochem. Biophys. Res. Commun. **339:**79–88.
32. **Padmanabhan, B., K. I. Tong, T. Ohta, Y. Nakamura, M. Scharlock, M. Ohtsuji, M. I. Kang, A. Kobayashi, S. Yokoyama, and M. Yamamoto.** 2006. Structural basis for defects of Keap1 activity provoked by its point mutations in lung cancer. Mol. Cell **21:**689–700.
33. **Ramos-Gomez, M., M. K. Kwak, P. M. Dolan, K. Itoh, M. Yamamoto, P. Talalay, and T. W. Kensler.** 2001. Sensitivity to carcinogenesis is increased and chemoprotective efficacy of enzyme inducers is lost in nrf2 transcription factor-deficient mice. Proc. Natl. Acad. Sci. U. S. A. **98:**3410–3415.
34. **Shibata, T., T. Ohta, K. I. Tong, A. Kokubu, R. Odogawa, K. Tsuta, H. Asamura, M. Yamamoto, and S. Hirohashi.** 2008. Cancer related mutations in NRF2 impair its recognition by Keap1-Cul3 E3 ligase and promote malignancy. Proc. Natl. Acad. Sci. U. S. A. **105:**13568–13573. (Erratum, **106:** 10393.)
35. **Shin, S., N. Wakabayashi, V. Misra, S. Biswal, G. H. Lee, E. S. Agoston, M. Yamamoto, and T. W. Kensler.** 2007. NRF2 modulates aryl hydrocarbon receptor signaling: influence on adipogenesis. Mol. Cell. Biol. **27:**7188–7197.
36. **Singh, A., V. Misra, R. K. Thimmulappa, H. Lee, S. Ames, M. O. Hoque, J. G. Herman, S. B. Baylin, D. Sidransky, E. Gabrielson, M. V. Brock, and S. Biswal.** 2006. Dysfunctional KEAP1-NRF2 interaction in non-small-cell lung cancer. PLoS Med. **3:**e420.
37. **Slitt, A. L., N. J. Cherrington, M. Z. Dieter, L. M. Aleksunes, G. L. Scheffer, W. Huang, D. D. Moore, and C. D. Klaassen.** 2006. trans-Stilbene oxide induces expression of genes involved in metabolism and transport in mouse liver via CAR and Nrf2 transcription factors. Mol. Pharmacol. **69:**1554–1563.
38. **Sykiotis, G. P., and D. Bohmann.** 2010. Stress-activated cap'n'collar transcription factors in aging and human disease. Sci. Signal. **3:**re3.
39. **Tarutani, M., S. Itami, M. Okabe, M. Ikawa, T. Tezuka, K. Yoshikawa, T. Kinoshita, and J. Takeda.** 1997. Tissue-specific knockout of the mouse Pig-a gene reveals important roles for GPI-anchored proteins in skin development. Proc. Natl. Acad. Sci. U. S. A. **94:**7400–7405.
40. **Thimmulappa, R. K., K. H. Mai, S. Srisuma, T. W. Kensler, M. Yamamoto, and S. Biswal.** 2002. Identification of Nrf2-regulated genes induced by the chemopreventive agent sulforaphane by oligonucleotide microarray. Cancer Res. **62:**5196–5203.
41. **Thimmulappa, R. K., C. Scollick, K. Traore, M. Yates, M. A. Trush, K. T. Liby, M. B. Sporn, M. Yamamoto, T. W. Kensler, and S. Biswal.** 2006. Nrf2-dependent protection from LPS induced inflammatory response and mortality by CDDO-imidazolide. Biochem. Biophys. Res. Commun. **351:** 883–889.
42. **Tong, K. I., A. Kobayashi, F. Katsuoka, and M. Yamamoto.** 2006. Two-site substrate recognition model for the Keap1-Nrf2 system: a hinge and latch mechanism. Biol. Chem. **387:**10–11.
43. **Wakabayashi, N., K. Itoh, J. Wakabayashi, H. Motohashi, S. Noda, S. Takahashi, S. Imakado, T. Kotsuji, F. Otsuka, D. R. Roop, T. Harada, J. D. Engel, and M. Yamamoto.** 2003. Keap1-null mutation leads to postnatal lethality due to constitutive Nrf2 activation. Nat. Genet. **35:**238–245.
44. **Watai, Y., A. Kobayashi, H. Nagase, M. Mizukami, J. McEvoy, J. D. Singer, K. Itoh, and M. Yamamoto.** 2007. Subcellular localization and cytoplasmic complex status of endogenous Keap1. Genes Cells **12:**1163–1178.
45. **Yamamoto, T., T. Suzuki, A. Kobayashi, J. Wakabayashi, J. Maher, H. Motohashi, and M. Yamamoto.** 2008. Physiological significance of reactive cysteine residues of Keap1 in determining Nrf2 activity. Mol. Cell. Biol. **28:**2758–2770.